Unavoidability and Functionality of Nervous System and Behavioral Randomness

Carlos M. Gómez *, Elena I. Rodríguez-Martínez and María A. Altahona-Medina

Department of Experimental Psychology, University of Seville, 41018 Seville, Spain; elisroma@us.es (E.I.R.-M.); maraltmed@alum.us.es (M.A.A.-M.)
* Correspondence: cgomez@us.es

Abstract: The basic functioning of the central nervous system is based on the opening and closing of ionic channels in the membranes of neurons. The behavior of ionic channels is considered to be a random process with an exponential probability distribution function. The central limit theorem implies that the mean of the sum of random variables generates a distribution in which the new variable tends to be normally distributed. The theorem implicitly implies that randomness can be embedded in a certain probability distribution but does not disappear. The present report will explore the possible implications for the functioning of nervous system and behavior of the constituent neural randomness. The possible functionality of "noise" to increase the exploratory space of nervous and behavioral systems will be considered.

Keywords: ionic channels; random process; psychometric function; geometric distribution; Gaussian distribution; threshold

1. Introduction

Behavioral and cognitive activities depend on electrophysiological neural activity based on ionic currents of chemical, mechanical and voltage membrane channels. Opening and closing of these channels are considered as probabilistic random processes and are modeled via an exponential probability distribution [1]. Open dwelling times follow a simple exponential model, but to model the closed channel interval, a sum of many exponential functions is needed. The quantal nature of synaptic vesicle liberation is another source of neural activity variability [2,3]. The stochastic activity of ionic channels would be an intrinsic source of randomness in the nervous system, while the random structure of stimulation would be another source of variability, i.e., in the case of light perception, the quantal nature of photon emission. The large number of ionic channels cannot override this intrinsic and extrinsic variability, and experimental evidence demonstrates that membrane potential presents fluctuations that affect the generation of spontaneous action potentials [4,5]. In situations in which neurons receive steady inputs, the inter-spike interval distribution shows broad variability [6,7]. During constant inputs, the exact time at which a given spike is generated reflects the internal noise more than the inputs that the neuron receives [8].

Given that behavioral and cognitive activities depend on the activity of neural networks activity, and given that those are dependent on the activity of individual neurons that, at a very basic level, depend on the probabilistic behavior of ionic channels, it can be inferred that high-order levels of brain function as cognitive and behavioral activities should show a stochastic component, given that operating with a combination of random variables preserves the random nature of the outcome. One important consequence of that is that the sum of the random variables is another random variable, which converges to the Gaussian distribution when N tends toward infinity: the so-called central limit theorem [9].

The present report tries to demonstrate that there are traces of random processes at the organismic level, as well as that a possible interpretation of that would be the successive alternation of geometric and Gaussian distribution across levels of integration in the central

nervous system. This would be achieved by reviewing the four different approaches followed by our group:

The lever press response of rats during variable interval schedules of reinforcement (VI) [10,11]; the fluctuations of the macroscopic activity of the abducens nerve [6], giving place to the ocular tremor; the perceptual changes during the observation of images in eye rivalry and ambiguous images [12]; and the psychometric (also called psychophysics) function [13]. The integration of unavoidable levels of neural randomness at the organismic level would facilitate flexibility in behavior [14].

2. The Inter-Response Time (IRT) Intervals in Variable Interval Schedules of Reinforcement

Animal behavior, although predictable in many instances, could also be considered to be unpredictable and modeled through stochastic processes. In fact, the reinforcement of certain responses (the increases in certain motor responses when generating positive outcomes in the subjects) in animal behavior would be a selective process on a pool of behavioral variability, in a similar manner to that in which it occurs in other biological systems such as evolutionary dynamics or the immune system [15,16].

Given the random structure of reinforcement in variable interval schedules of reinforcement (VI), the animal lever press in VI schedule of reinforcement would be particularly suited for modeling and analyzing random processes. In VI, there is a variable time for a response to be reinforced, and the response reinforced can occur at any time in the interval, following a scheduled random pattern inside the interval. In a VI with a 60 s period, the reinforced response occurs at any time in this period, as selected by random number generators in the Skinner box controller program. In this study [10], it was checked if stochasticity appears in the response behavior of rats in VI schedules by computing the autocorrelation function and the probability density function of the IRTs. In fact, the IRT series showed no autocorrelation, as tested through autocorrelation values inside the so-called Bartlett bands (Figure 1).
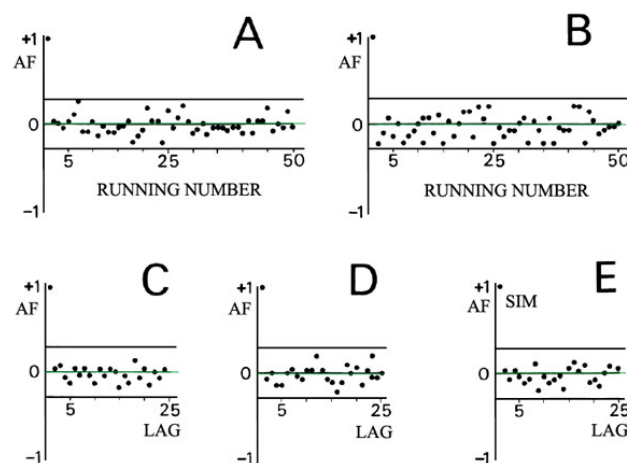
Figure 1. Autocorrelation function (AF) of the individual IRT values (**A**,**B**) and cumulated IRT values in time bins (**C**,**D**). The same for randomly generated IRT values (**E**). Notice that autocorrelation values are always inside the Bartlett bands, indicating no time dependency in the IRT series. Adapted with permission from [10]. 1992, Springer.

These statistical results can be interpreted as if the IRT series could be modeled via a random process with no time serial structure [17]. The latter analysis suggests that an internal non-periodic process underlies the decision process of lever response during VI. In this case, it is possible that, as suggested by Staddon and Simmelhag [15], the inner behavioral dynamics would profit from using a random internal generator to adaptively adjust its behavior to the unpredictable VI schedule of reinforcement. Interestingly, the

IRT frequency distribution was modeled as a gamma and/or a Poisson distribution, both distributions considered as distributions modeling random events:

The gamma distribution following Johnson and Kotz [18] is modeled as follows:

$$Px(X) = \frac{(X-y)^{\alpha-1} \cdot e^{-(X-y)/\beta}}{\beta^{\alpha} \cdot \Gamma(\alpha)} \tag{1}$$

Alpha = arithmetic mean/2 * (arithmetic mean − geometric mean)
Beta = arithmetic mean/Alpha.
y = when n is large, it is reasonable to estimate y as a value smaller than the smallest observed value [18].

And

$$\Gamma(\alpha) = \int_{o}^{\infty} t^{\alpha-1} \cdot e^{-t} dt \tag{2}$$

The mean/variance ratio close to 1 (Fano factor) suggested that the IRT time series could be distributed as a Poisson process. The Poisson probability density function is defined [19] as follows:

$$P(X = x) = e^{-h} \cdot h^{x}/x! \tag{3}$$

The quantity h is the only parameter of the distribution and can be estimated as the variance or the mean of the data. And x is the number of events in a certain time or space. Both distributions fit the IRT values, although the Poisson distribution did so in a significant manner in a higher percentage of cases than the gamma distribution (90% and 60% of cases, respectively).

Given that a Poisson probability density function represents the probability that a random variable appears n times in a fixed period of time or space [19], as well as that the gamma probability density function of IRT in this context would be generated as produced by the counting of n events from a random variable, both models of IRTs are based on random variables. The latter observation, joined to the previous comment about the lack of a time serial structure, points to the idea that IRTs in VI behavioral reinforcement schedules could be modeled as random variables. From this perspective, learning would permit us to reduce non-adaptive random responses and amplify adaptive random responses [15,20].

3. Ocular Tremor

The ocular tremor is a micromovement of the eye (several min of arc). This tiny movement has been proved to be functional to prevent vision fading, which can be produced by the adaptation of photoreceptors if the light entering the eye is static during eye fixations [21]. The tiny tremor ensures that a given photoreceptor would receive constant light in terms of intensity and quality [22], avoiding adaption and vision fading. The purpose of this study [7] was to demonstrate that the statistical properties of the neural activity of the extraocular muscles were the cause of this movement, after filtering neural activity through the ocular mechanics. Taking into account the possible stochastic nature of the behavior of abducens motoneurons [6], as well as the fact that the statistical properties of the spike count of the abducens nerve [7] would also be a random process due to the central limit theorem, then a random behavior for the ocular tremor movement is implied. Notice that ocular tremor movement is caused by the activity of the extraocular muscles as a by-product of the oculomotor nerves.

This endeavor was possible given the large amount of data about the activity of individual motoneurons in the abducens nucleus and nerve [6,23]. The abducens nucleus and nerve control the lateral rectus muscle, which controls the eye's outward direction (abduction), while the motoneurons of the oculomotor nucleus control the inward direction (adduction). The here-reviewed simulation only took into consideration neural spiking at the abducens nerve, assuming that the activity of the oculomotor nerve would be symmetric to the pattern of activity of the abducens nucleus, and then both would achieve a similar result. Therefore, the objective of the simulation of the abducens nerve was

recreate possible global activity during eye fixations to define if there was any serial time dependency (rhythmic activity), as well as to compute the possible effects of the abducens neural activity in the eye position, and then determine if a pattern similar to this pattern of ocular tremor was replicated.

Figure 2 shows the procedure followed to compute the spiking rate of the abducens nerve from the sum of the spikes generated by individual neurons (Figure 2A). The parameters used for computing the spike train for each neuron are described in Table 1 of Gómez et al. [7] and depicted in Figure 2A. The abducens nerve global activity was computed as the sum of the spike trains of individual motoneurons (Figure 2B). The frequency distribution of the global activity was fitted by a Poisson distribution, despite resembling a Gaussian distribution when a high number of neurons were active, as occurs for the more eccentric positions. Then, the Power Spectral Density (PSD) of the spiking global activity carried by the abducens nerve was computed for different eye positions (Figure 3A,C), producing a rather flat spectrum (Figure 3A), being flat for high frequencies and peaking at the mean frequency of motoneuron activity for a given eye position (Figure 3B). A final analysis was performed to observe the spectrum of the eye position. The PSD function of eye position falls monotonically with frequency due to the filtering of the ocular mechanics model, but for the eccentric position of the eye, a peak remained at the same mean frequency as the motoneurons (Figure 3D).
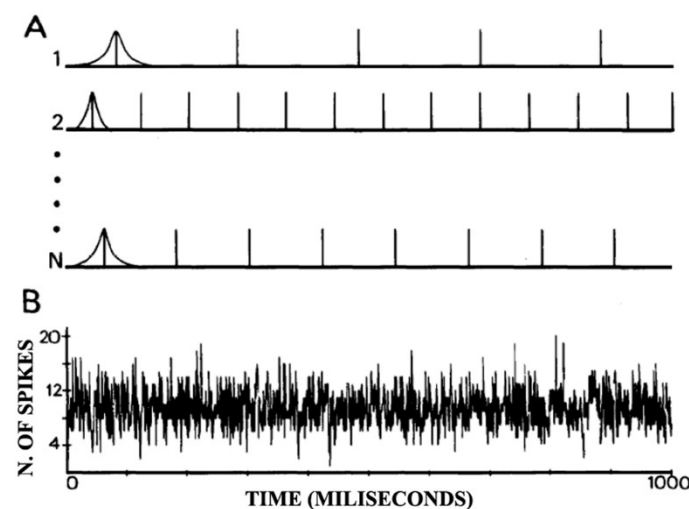
Figure 2. Computation of the total activity of the abducens nerve. (**A**) The activity of three motoneurons of the left abducens nucleus during eye fixation. The clock-like firing activity is modulated by random noise following a normal distribution. (**B**) The simulation of the neural discharge carried by the abducens nerve for a central position of the eye in the orbit computed as the sum of the spike trains of single neurons. Adapted with permission from [7]. 1989, Elsevier.

To compute the PSD of eye tremor (Figure 3B,D), the PSD of the simulated abducens nerve spike count was filtered using a model of the ocular mechanics (following Robinson [24]) by multiplying the latter neural signal by the squared transfer function (TFz) of the second-order differential equation modeling ocular mechanics.

$$\text{TF}^2 = 1/((1 + 2\pi f \cdot \text{T1})^2) \cdot (1 + 2\pi f \cdot \text{T2})^2) \tag{4}$$

T1 and T2 were calculated from empirical data providing the position, velocity, and acceleration coefficients (k, r, and m, respectively) of the second-order differential equation modeling the ocular mechanics:

$$R(t) = R0 + k \cdot \text{Pos} + r \cdot d\text{Pos}/dt + m \cdot d\text{Pos}^2/dt^2 \tag{5}$$

R(t): Force exerted by the muscle (function of abducens nerve discharge);

R0: Constant;
Pos: Eye angular position;
dPos/dt: Eye angular velocity;
$dPos^2/dt^2$: Eye angular acceleration.

Then, T1 was calculated as r/k and T2 as m/k.
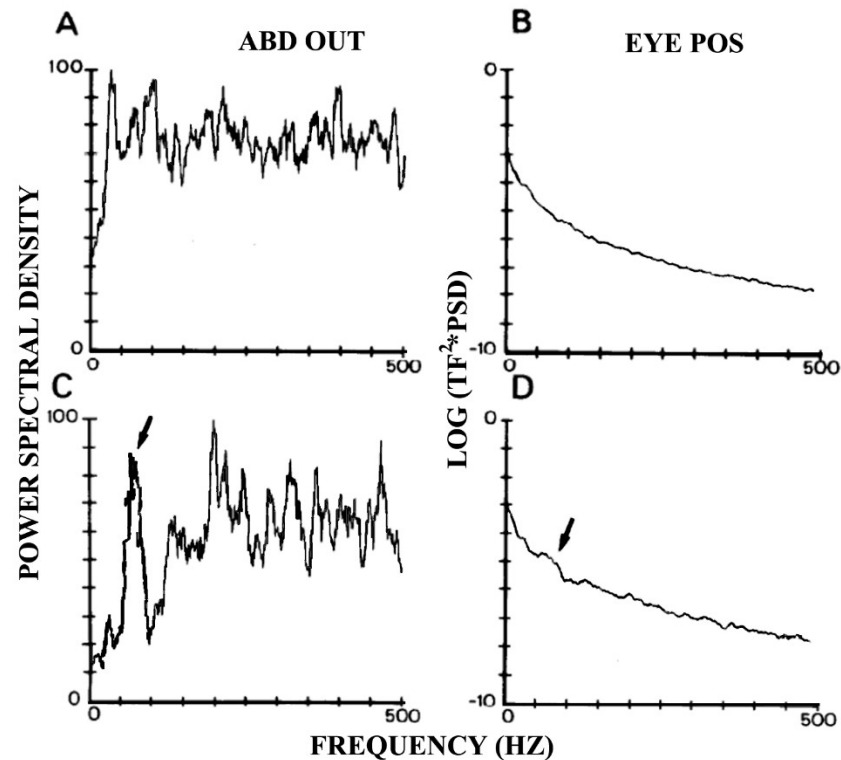
Figure 3. Power Spectral density. (**A**,**C**) Averaged Power Spectral Density (PSD) of 50 sequences of the simulated neural discharge of the abducens nerve (ABD OUT) for $0°$ (**A**) and $10°$ eye positions (**C**). (**B**,**D**) PSD functions of the $0°$ (**B**) and $10°$ eye positions (EYE POS) (**D**). Adapted with permission from [7]. 1989, Elsevier.

Apart from the demonstration in the present report that the ocular tremor would be produced by the statistical properties of the oculomotor nerves, given the objective of the present report, it is important to consider that at the organismic level, there are traces of random neural noise activity, so it can be proposed that the deviations from the strict pacemaker activity of abducens neurons (following a normal distribution), producing a relatively flat frequency spectrum of the neural nerve discharge, except for the mean of the neural discharge of neurons in a certain eye position, would be an indication of a random process in the global activity of the macroscopic abducens cranial nerve. This suggestion can also be sustained by the Poisson distribution of the nerve spike discharge, approaching a Gaussian distribution as the number of active motoneurons increases.

4. The Perceptual Transitions during the Perception of Ambiguous Figures and Eye Rivalry

During perception of ambiguous figures such as the Necker cube, as well as the perception of incompatible images presented in each eye (eye rivalry phenomenon), the conscious perceptions of the two incompatible images alternate. It is possible, given the broad variability in the perceptual duration of the presented images, that transitions between percepts would be animated via random processes. In fact, at least two models have proposed such random influence at the organismic behavioral level. Logothetis [25] proposed that perceptual duration histograms are fitted by gamma distributions and Lehky [26] by a log-normal probability. Lehky [26] also showed that the time series

presented no autocorrelations and that this time series was not explained by a chaotic system. The demonstration of not being a chaotic system was based on the correlation dimensions and nonlinear forecasting of the time series, giving ground for a random process to govern the transitions of perceptual states. Gómez et al. [12] proposed that alternation between percepts occurs as a form of competition between the neural networks representing the two percepts. Such networks should have a mutual inhibition, as depicted in Figure 4A, and each network representing an image should have a stochastic dynamic, as represented in Figure 4B.
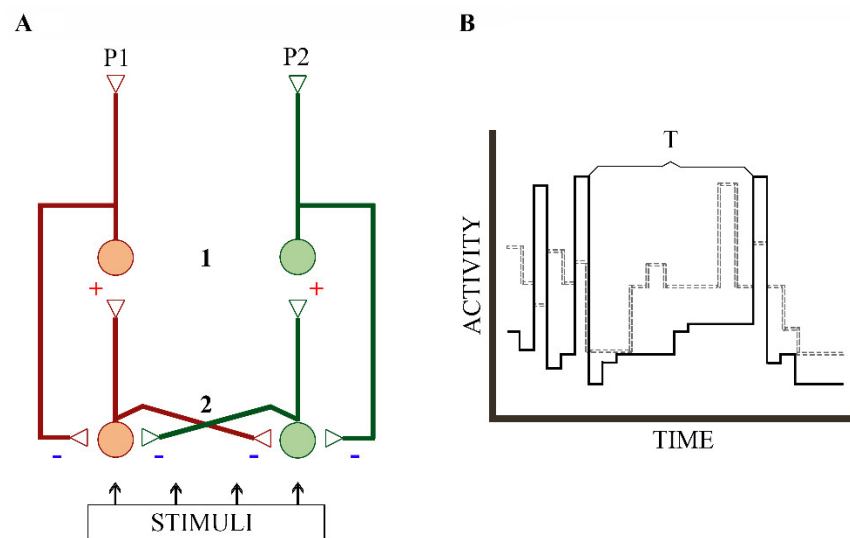
Figure 4. Competition model for the perception of ambiguous figures and eye rivalry. (**A**) Two independent networks that are competing (mutually inhibiting each other) to emerge in the perceptual field (P1 and P2). 1 represents the conscious perceptual level and 2 the sensory processing level. (**B**). Only the network presenting the higher activity would reach the perceptual threshold, with T representing the conscious perception of the network represented by the dotted line.

The competitive model assumes that the expression of a given percept occurs when the activity of its underlying neural network obtains a value higher than that of the alternative network [27]. The probability p is estimated such that the network that allows the representation of a certain percept wins the competition, and (1 − p) is the probability of the opposite percept winning the competition.

Then, the frequency of cases in which a certain percept lasts a certain duration (f(t)): Duration Time) obtains a particular value between time 0 and time t, which is as follows:

$$f(t) = (1 - p)^{(t - 1)} \cdot p \cdot N \tag{6}$$

This equation implies that the frequency of cases in which a perception time obtains a particular value (f(t)) depends on how many times it wins the competition on a time scale between t = 1 and t. Equation (6) corresponds to the geometric probability density function (Figure 5A) multiplied by the number of individual perceptions (N).

f(t) = frequency: The number of times a perception lasts a period of t (N = total number of individual perceptions).
$(1 - p)^{(t - 1)}$ = The probability that the current percept network wins the competition. It must be multiplied by N to obtain the frequency histogram of the duration of a percept.
p: the alternative percept);
t − 1 = The number of times that the network of one of the percepts wins in a row and current perception is maintained
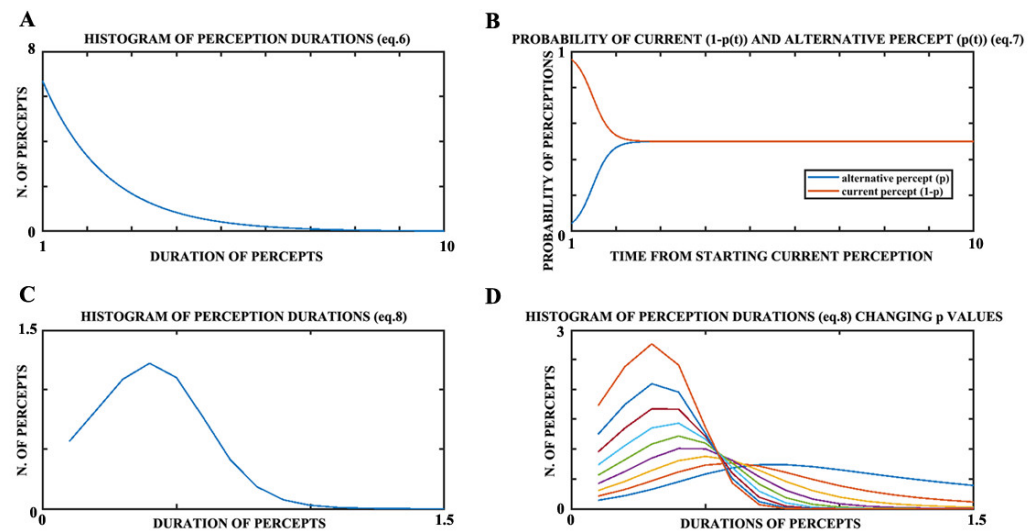
Figure 5. Durations of perceptions with p = 0.5. (**A**) Frequency histogram of perception durations following a geometric distribution (Equation (6)). (**B**) Change in p values with time elapsed from the previous perceptual change (Equation (7)). (**C**) Frequency histogram of perception durations following a geometric distribution, modulating p as a function of the time elapsed from the previous perceptual change (p(t)) (Equation (8)). (**D**) Same as (**C**) but changing p values from 0.1 to 0.9.

The values of $(1 - p)$ and p can be made to be dependent on the time in which the transition occurs. This modification of the geometric distribution permitted us to increase the fitting of experimental data [12] and supposes, that after a transition, there is a higher probability for the network representing the current perceived object to be defeated in the competition. Equation (7) and Figure 5B imply that the average probability that the win probability of the neural network representing the alternative percept (p) relative to the one that won the competition $(1 - p)$ increases over time, while the probability that the current perception would be defeated in the competition increases with time. The most probable physiological mechanism would be the habituation of the neural network representing the current perception. Therefore, the probability that a percept is consciously perceptible during a certain time will be a function of the time since its perception was established (Equation (8)). Therefore, the probability of perception is now a function of time since the last change in perception in this bistable perceptual system (p(t)) (Figure 5B).

$$p(t) = (1/(1 + (e^{\wedge}((-t \cdot A) + e^2)))) \cdot p \tag{7}$$

A = A parameter used to modulate the curvature of the sigmoid;
e^2 is introduced into the sigmoid equation to have the origin at zero.

Finally, the frequency distribution of perception times (Figure 5C) should be

$$f(t) = (1 - p(t))^{(t-1)} \cdot p(t) \cdot N; \tag{8}$$

The parameter A must be estimated from the empirical distribution of f from time 0 to the mode of the empirical distribution of f. To estimate the parameter p, only the right tail of the f distribution will be considered, because in this part of Equation (7), p(t) and $(1 - p(t))$ have reached the asymptotic level, and p(t) has a value close to the asymptotic value p.

The fitting of this model was successful for fitting the frequency histograms of the perceptual times of both the Necker cube and eye rivalry [12]. Interestingly, the mean time of perception was modulated by attention. This experimental result can be accommodated in the model by modulating the value of parameter p (Figure 5D), which changes the shape of the frequency histogram of perception durations. The latter finding suggests that

attention, a higher cognitive function, is able to modulate the neural activity of a given representational network.

The model has also been successfully applied to another situation: the behavior of the lever pressing in the VI schedule of reinforcement [11]. In this approach, the same model is applied to motor networks representing the lever pressing (p), as well as any other possible alternative behavior ($1 - p$). The use of this modified geometric distribution (with the parameter p being dependent of time) would be an alternative to the gamma and Poisson distributions for fitting the IRTs, as previously described [10]. This fitting approach would not only highlight the random process for the IRTs, but it would also be based on the competition between the lever pressing behavior and any other possible behavior, in a similar manner to the competition between alternative percepts in ambiguous figures and eye rivalry.

5. The Psychometric Function (Also Called Psychophysics Function)

According to the America Psychological Association, this function refers to "the relationship between a stimulus and judgments about the stimulus, as expressed in a mathematical formula". The relationship between the intensity of the stimulation and the probability of reaching the perceptually conscious threshold is described by an asymptotic sigmoid [28]. This relationship indicated a continuous increase in the probability of perception with stimulus intensity increase.

One possibility of generating such probabilistic perceptual threshold would be related to the neural noise of sensory channels, in which, on certain occasions, the external energy is sufficient for reaching the threshold, or not in other cases. The probabilistic threshold would be more critical for low-intensity sensory stimulation, in which the intensity of neural noise can be critical for reaching the perceptual threshold. This possibility is exemplified by the phenomenon of stochastic resonance, which refers to the fact that the addition of a certain amount of noise leads to better information transmission [29]. In the case of low-intensity stimuli, stochastic resonance would facilitate reaching the perceptual threshold.

This study tried to explain the probabilistic nature of the psychometric function as a consequence of the random behavior of voltage-gated ionic channels. The approach followed tried to capture the stochastic nature of the perceptual threshold based on neural noise, without entering into an almost impossibly detailed description of the process in neurons and neural assemblies but keeping the essentials of the already-demonstrated threshold process approach, which holds for ionic channels, action potential generation, and the perceptual threshold. This approach permits the exclusion of many of the mechanistic details, without losing the dynamic essentials. In fact, the influence of neural noise on the discharge of neurons [8], as well as the influence of noisy spike trains on perception [30] has already been addressed. The simulation, best defined as numerical exploration, brought from the random opening of ionic channels to the psychometric function is described in Figures 6–8 (details in Gómez, [13]).

Figure 6A shows a series of simulated closings and openings of ionic channels selected from a Bernoulli random process. The frequency histogram of the opening durations of an ionic channel is displayed in Figure 6B, showing an exponential decay, as has been observed empirically [1]. The time series of the number of open channels are represented in Figure 6C for three different stimuli intensities. This time series presents a Gaussian distribution (Figure 6D). The increase in the number of open channels for higher stimuli intensity induced an increase in variability (Figure 6E,F).
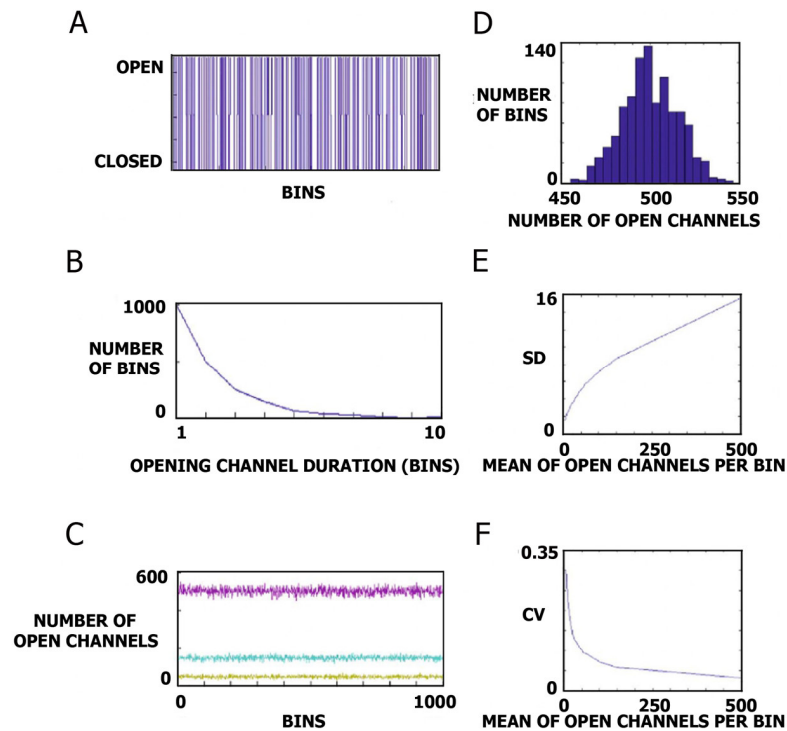
Figure 6. Simulation of ionic channel behavior. Series of openings and closings of an individual ionic channel modeled by a Bernoulli random process (**A**). (**B**) Exponential-like decay of the ionic channel opening durations. (**C**) Time series of the number of ionic channels open at different stimulus intensities. (**D**) Bell-shaped distribution of the number of open channels per time bin. (**E**) Increase in absolute variability (Standard Deviation: SD) and decrease in relative variability (coefficient of variation: CV) (**F**) with the number of open channels. Adapted with permission from [13]. 2008, Springer.
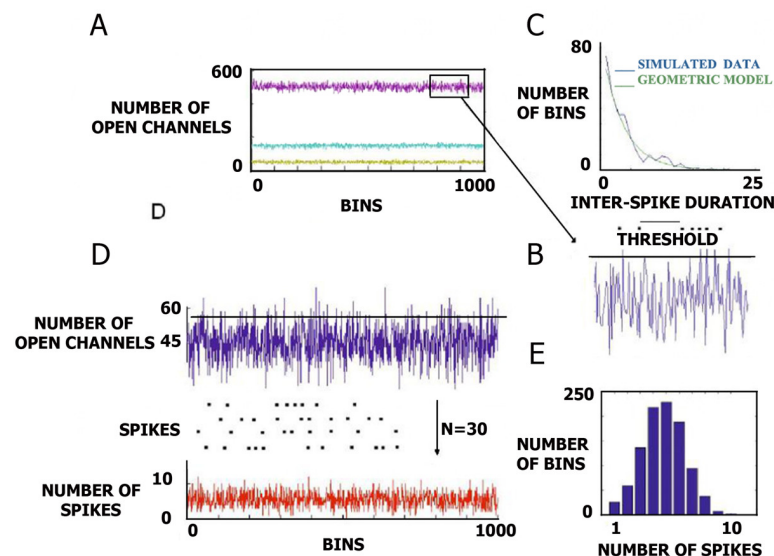
Figure 7. Simulation of the number of spikes in a sensory network representing a perceptual object. (**A**) Same as in Figure 6C. (**B**) The number of open channels in each time bin with a line indicating the hypothetical action potential threshold. (**C**) The geometric model of the frequency distribution of the inter-spike intervals. (**D**) On the upper side, the open channel time series, and on the middle and lower sides, the number of spikes in the sensory network that would represent the perceived object. (**E**) Gaussian-like distribution of the number of spike series of the lower (**D**). Adapted with permission from [13]. 2008, Springer.
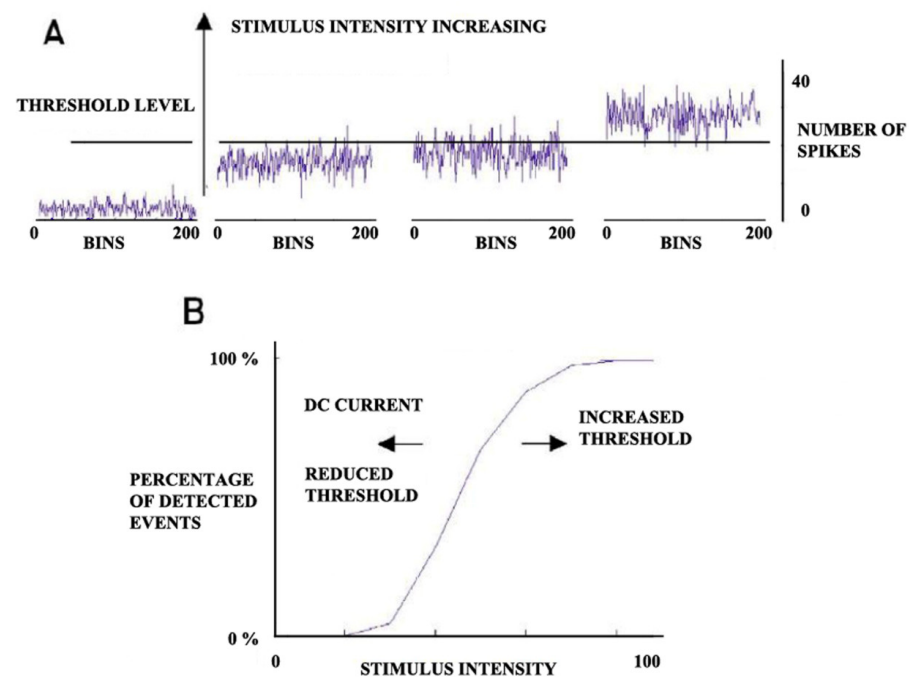
Figure 8. Psychometric or psychophysics function. (**A**) Number of spikes for the increasing intensity of the stimulation. The line shows the arbitrary threshold for stimulus detection. With stimulation intensity, the number of spikes per time bin increases and then the event detection probability also increases. (**B**) Psychometric or psychophysics function. The predicted displacement of the psychometric function caused by reducing or increasing the threshold for event detection or injecting a certain level of DC current is indicated by arrows. Adapted with permission from [13]. 2008, Springer.

Although the relative variability in the number of open channels per time unit decreases with the number of open channels (measured as a coefficient of variation) (Figure 6F), the absolute variability measured as the standard deviation increases monotonically with the number of ionic channels and, consequently, with the stimulus intensity (Figure 6E). The important point in the simulation of the opening and closing of the channels, modeled via a random Bernoulli process, is that the addition of the channel does not ride out the neural noise intrinsic to the neuron, and then the neuron discharge to a constant current input is also influenced by neural noise. This is shown in Figure 7. Figure 7A shows the time series of the number of ionic channels openings induced by a stimulus near the threshold. The number of open channels per time bin appears in Figure 7B. The line indicates the neuron fixed threshold for inducing an action potential. As a consequence of the imposed threshold and the number of open channels, spikes are generated. Figure 7C shows the frequency distribution of the inter-spike interval obtained. The results for the frequency distribution of the inter-spike intervals conform to the expected geometrical distribution, similar to Equation (6), which, in this case, is as follows:

$$\Pr\left(X = t\right) = \left(1 - p\right)^{t-1} \cdot p \tag{9}$$

Therefore, the probability of the duration of a given inter-spike interval (X) having a value (t) is equal to the probability of the number of open channels being equal to or above the threshold in a certain time bin (p). Then, p must be multiplied by the probability that in the (t − 1) previous time bins, the number of open channels had a value lower than the threshold value (1 − p). Figure 7D shows the number of spikes in a neural network representing the stimulus (below), and Figure 7E shows the bell-shaped frequency distribution of the number of spikes by time unit. The last part of the simulation tries to obtain the psychometric function using a fixed perceptual threshold of the number of

spikes in the neural net representing the presented stimulus. Figure 8A shows the time series of the total number of spikes relative to the increasing intensity of the stimulus, and in Figure 8B, the psychometric function is obtained by plotting the frequency of cases in which the number of spikes is higher than the perceptual threshold.

The whole model can be validated at the different levels of description from ionic channels to the psychometric function; I would concentrate here on the psychometric function. The validation of more basic levels can be found in the original publication [13]. The obtained shape in the simulation is similar to the sigmoid psychometric function obtained experimentally [31,32]. The simulation is able to predict the direct current injection of cortical columns representing the direction of moving targets' bias psychometric function to lower stimulus intensities (Figure 8B) [33]. The latter experiment would be, in some sense, an electrophysiological substitute for attention to certain stimuli, which also reduce the perceptual threshold [34]. By increasing the amount of noise, it was possible to bias the sigmoidal psychometric function with a perceptual improvement similar to "stochastic resonance" [29]. Interestingly the stochastic resonance results open the possibility that reducing the threshold for a certain stimulus through attention could possibly be implemented not only via stochastic resonance but also by the increase in the neural activity arriving at the neural net representing the observed percept [34].

From the perspective of the present review, the main point of this numerical exploration is that, at least at a theoretical level, the neural noise activity cannot be ridden out, and it can be observed at a macroscopic perceptual level.

6. Discussion

The aim of this report was to demonstrate that the probabilistic natures of the basic electrophysiological processes of neurons can still be observed at the level of the organism. It must be always considered that given the huge complexity of biological processes, we can only suggest that random modeling is a good approximation of the studied phenomenon, but it is very difficult, if not impossible, to overlook the fact that some hidden or unknown variables are deterministically defining the process at hand. Also, the distinction between chaotic and random behavior is very difficult [26]. The approach followed in the different studies presented here is (i) to model the data via probability density functions, which, theoretically, are the by-products of random processes, and (ii) show no time dependence in the data time series.

The latter two characteristics are the main properties of random processes [9] The neural global discharge of the abducens nerve [7] and the IRTs of lever pressing in a VI schedule of reinforcement fulfilled both conditions. The perception times of ambiguous figures and eye rivalry [12] were fitted by the modification of the geometric distribution, and. qualitatively, there were no time dependencies in the successive events. The obtained psychometric function was based on a simulation in which the organismic response (the psychometric or psychophysics function) was constructed from its more basic underpinnings [13], in the interaction between the stimulus intensity and the random closing and opening of ionic channels. We will comment first on the psychometric function study given its more detailed description extending from the molecular to the organismic level.

The results of the simulation of the psychometric function could lie in the stochastic nature of voltage-gated ionic channels. The computation of a probabilistic psychometric function suggests that variability at the microscopic level is conserved at the perceptual organismic level. An interesting point derived from the simulations is the alternation between geometric, exponential, and Gaussian distribution across levels: exponential for the opening time of channel distributions (please notice the great similarity between geometric and exponential distributions), Gaussian for the number of channels open at a given time, geometric for the inter-spike time intervals of single neurons, and Gaussian for the number of spikes in the neural net representing the perceptual level. Finally, and as a result of the whole process, the sigmoidal shape of the psychometric function, as a consequence of the collective behavior of sensory modules was obtained from the last level

of representation: the number of spikes in the neural net representing the percept that reached the perceptual threshold (i.e., [30]).

The exponential and geometric distributions would be obtained from a threshold process on a random variable. Here, the random variable, which can be proposed to underlie the consecution of a voltage sufficient for overriding the energy barrier for the transitions between closed and open ionic channels, would be the thermally induced local movement of ions in the vicinity of the channels. In fact, the voltage and ion concentrations in ionic solutions possibly follow an Ornstein–Uhlenbeck process, with a mean voltage value due to the ion concentration of intra- and extracellular medium and random processes due to the thermal noise and electromagnetic interactions between ions and other ions or water. It is expected that the voltage at a given position should be random due to the Brownian motion of ions in the extra- and intracellular fluid.

Therefore, it can be speculated that a certain concentration of ions due to largely random electrochemical processes could create an electric field across the ionic channel to determine its opening. In fact, it is not strictly necessary for the fluctuation of voltage across ionic channels to have any particular distribution, just that it reaches a certain threshold to induce the channel opening. The geometric distributions of the inter-spike intervals would be obtained from the Gaussian distribution of intracellular voltages created from the normal distribution of open channels per time unit, from which, once a certain threshold is obtained, spikes are generated. The latter argument is supported by more detailed simulations in which subthreshold voltage fluctuations increased with the mean voltage and the neuronal noise was normally distributed [35]. The Gaussian distributions obtained for the number of open ionic channels and the number of spikes in the neural network representing the percept would be a direct consequence of the central limit theorem.

Therefore, a succession of distributions across levels of integrations would represent a Gaussian distribution of voltage around channels, an exponential (may be geometric given the shape similarity with the exponential distribution) distribution for the opening times of channels, a Gaussian distribution for the intracellular voltages of neurons, a geometric distribution for inter-spike intervals, and a normal distribution for the global number of spikes in the network representing the percept. An interesting prediction for the model would be that for a stimulus of low intensity, the time intervals between two perceived stimuli should follow a geometrical distribution. With respect to the probability density functions of the different variables presented in this review, the perceptions of ambiguous figures [12], IRTs [10,11], and abducens nerve spike count [7] were all tested via chi-squared and Kolmogorov–Smirnov tests. However, for the simulation of the psychometric function [13], only an approximate graphical method was applied.

The Gaussian distribution for the global activity of a neural structure in response to a continuous input was validated by the computation of the number of spikes in the abducens nerve at the neuronal level, and the abducens motoneurons show a Gaussian distribution [6]. However, for constant inputs, Poisson distributions [36,37] and unimodal left-skewed distributions [38] have been obtained. This variety of probability distributions for inter-spike intervals can be explained by changes in ionic conductances after spikes, not only producing phenomena such as after-hyperpolarization potential [39,40] but also producing short- and long-range adaptation and the activation of recurrent neural activity through reverberant circuits. Therefore, it is not surprising that during neuronal steady inputs, different empirical inter-spike frequency distributions are obtained in neuron discharge.

With regard to the duration of perception in eye rivalry and ambiguous figures [12] and the IRTs of lever pressing in VI [11], both were explained by the geometric distribution and refractoriness for very short durations due to the change in the probabilities as a function of time from the preceding event (perception or response). Perception durations did not show qualitatively long-range time series dependency, and the IRTS proved by means of autocorrelation the absence of time dependency.

The possible random behavior for ambiguous figures' perceptual changes over chaotic deterministic dynamics has previously been explored [26], and for ocular tremor and the psychometric function, the compelling argument that the constituents of the model are random processes (inter-spike modeling and the opening and closing of ionic channels, respectively) suggest a random basis for these organismic phenomena. But, of course, it does not discard other alternative models based on deterministic chaotic dynamics. In the case of IRT, probability density functions have been fitted to the data and no time dependence in the data time series has been found. Although these results suggest random behavior, more compelling evidence, as this suggested by Lehky [26], is needed.

By integrating all the previous data, it can be proposed that at the organismic level, there are clear traces of random processes, probably due to the random basic electrophysiological processes of neurons. It has been proposed that the presence of this unavoidable random activity would be used by organisms to generate behavioral variability that could be used to reinforce the most adaptive behaviors, as in other selective systems such as species evolution [41], clonal selection in the immune system [42], or neural network selection in the so-called "selection of neuronal groups theory" [43]. In the present report, the notion of alternation across levels of Gaussian distributions (ion-mediated microscopic voltage distributions, intracellular voltages mediated by ionic channels, global activity in macroscopic structures such as the abducens nerve), as well as geometric distributions (and exponential distributions) mediated by a threshold to be overcome (ionic channels opening, spike firing, perception and responses), would be a functional characteristic in the transition from the microscopic to the macroscopic in the nervous system. It must be highlighted that the stance taken in the present report is to consider that the presence of thermal noise in the ionic channels and ionic solution across the membrane does not constitute just hidden variables but also intrinsic noise in which the neurons, networks, and behavior have to co-live and somehow thrive for generating behavioral flexibility [44,45]. In this sense, neural and behavioral variability would be caused not only by complex neural dynamics [45] but also by intrinsic neural random processes. The phenotypical variability in life is huge for the organization levels presented in this review, as well as in any other order of complexity level of life. We have tried only to highlight the influence of neural noise based on biophysical concepts of behavioral variability. Future studies should delimitate the relative importance of each of the factors influencing behavioral freedom of degrees in similar sensory contexts.

Author Contributions: Conceptualization, C.M.G.; resources, C.M.G., E.I.R.-M. and M.A.A.-M.; writing—original draft preparation, C.M.G., E.I.R.-M. and M.A.A.-M.; writing—review and editing, C.M.G., E.I.R.-M. and M.A.A.-M.; funding acquisition, C.M.G. and E.I.R.-M. All authors have read and agreed to the published version of the manuscript.

Funding: This work was supported by the Spanish Agencia Estatal de Investigación (AEI) (PID2022-139151OB-I00) (FEDER funds), and the Consejería de Innovación, Ciencia y Empresa of the Junta de Andalucía (P20_00537).

Institutional Review Board Statement: Not applicable.

Informed Consent Statement: Not applicable.

Data Availability Statement: The original contributions presented in the study are included in the article, further inquiries can be directed to the corresponding author.

Conflicts of Interest: The authors declare no conflict of interest.

References

1. Hille, B. *Ion Channels of Excitable Membranes*, 3rd ed.; Sinauer Associates: Sunderland, UK, 2001; ISBN 978-0878933211.
2. Del Castillo, J.; Katz, B. Quantal components of the endplate potential. *J. Physiol.* **1954**, *124*, 560–573. [CrossRef] [PubMed]
3. Destexhe, A.; Rudolph, M.; Fellows, J.M.; Sejnowski, T.J. Fluctuating synaptic conductance recreate in vivo-like activity in neocortical neurons. *Neuroscience* **2001**, *107*, 13–24. [CrossRef] [PubMed]

4. Strassberg, A.F.; De Felice, L.J. Limitations of the Hodgkin–Huxley formalism: Effect of single channel kinetics on transmembrane voltage dynamics. *Neural Comput.* **1993**, *5*, 843–855. [CrossRef]

5. Chow, C.; White, J. Spontaneous action potentials due to channel fluctuations. *Biophys. J.* **1996**, *71*, 3013–3021. [CrossRef] [PubMed]

6. Gómez, C.; Canals, J.; Torres, B.; Delgado-García, J.M. Analysis of the fluctuations in the inter-spike of abducens nucleus neurons during ocular fixations in the alert cat. *Brain Res.* **1986**, *381*, 401–404. [CrossRef]

7. Gómez, C.; Quero, J.M.; Escudero, M. Computer simulation of the neural discharge carried by the abducens nerve during eye fixation in the cat. *Int. J. Biomed. Comput.* **1989**, *24*, 207–215. [CrossRef] [PubMed]

8. Schneidman, E.; Freedman, B.; Segev, I. Ion channel stochasticity may be critical in determining the reliability and precision of spike timing. *Neural Comput.* **1998**, *10*, 1679–1703. [CrossRef]

9. Pishro-Nik, H. *Introduction to Probability, Statistics and Random Processes*; Kappa Investigación, LLC: Miami, FL, USA, 2014; ISBN 978-0990637202.

10. Gómez, C.; Ruiz-Adán, A.; Llosa, M.; Ruiz, G. Quantitative Analysis of IRT Variability during the First Training Stages of a Variable-Interval Schedule in Rats. *Psychol. Rec.* **1992**, *42*, 273–284. [CrossRef]

11. Gómez, C. A Competition Model of IRT Distributions during the First Training Stages of Variable-Interval Schedule. *Psychol. Rec.* **1992**, *42*, 285–293. [CrossRef]

12. Gómez, C.; Argandoña, E.D.; Solier, R.G.; Angulo, J.C.; Vázquez, M. Timing and competition in networks representing ambiguous figures. *Brain Cogn.* **1995**, *2*, 103–114. [CrossRef]

13. Gómez, C.M. Numerical exploration of the influence of neural noise on the psychometric function at low stimulation intensity levels. *J. Biosci.* **2008**, *33*, 743–753. [CrossRef]

14. Waschke, L.; Kloosterman, N.A.; Obleser, J.; Garrett, D.D. Behavior needs neural variability. *Neuron* **2021**, *109*, 751–766. [CrossRef]

15. Staddon, J.E.R.; Simmelhag, B. The superstition experiment: A reexamination of its implications for the principles of adaptative behavior. *Psychol. Rev.* **1971**, *78*, 3–43. [CrossRef]

16. *Laszlo, L The System View of the World*; Braziller: New York, NY, USA, 1972; ISBN 9780807606360.

17. Gottman, J.M. *Time-Series Analysis. A Comprehensive Introduction for Social Scientists*; Cambridge University Press: London, UK, 1981; ISBN 9780521235976.

18. Johnson, N.I.; Kotz, S. *Continuous Univariate Distributions-1*; Houghton Mifflin Company: Boston, MA, USA, 1970.

19. Sokal, R.R.; Rohlf, F.S. *Biometry*; W. H. Freeman: New York, NY, USA, 1981.

20. Deneubourg, J.L.; Aron, S.; Goss, S.; Pasteels, J.M.; Duerinck, G. Random behavior, amplification processes and number of participants: How they contribute to the foraging properties of ants. *Physica* **1986**, *22D*, 176–186.

21. Carpenter, R.H.S. *Movements of the Eyes*; Pion: London, UK, 1977.

22. Steinman, R.M.; Haddad, G.M.; Skavensky, A.A.; Wyman, D. Minature eye movement. *Science* **1973**, *181*, 810–819. [CrossRef]

23. Delgado-Garcia, J.M.; del Pozo, F.; Baker, R. Behavior of neurons in the abducens nucleus of the alert cat. I. Mononeurons. *Neuroscience* **1986**, *17*, 929–952. [CrossRef]

24. Robinson, D.A. The use of control systems analysis in the neurophysiology of eye movements. *Annu. Rev. Neurosci.* **1981**, *4*, 463–503. [CrossRef]

25. Logothetis, N.K. Vision: A window on consciousness. *Sci. Am.* **1999**, *281*, 69–75. [CrossRef] [PubMed]

26. Lehky, S.R. Binocular rivalry is not chaotic. *Proc. Biol. Sci.* **1995**, *259*, 71–76. [CrossRef] [PubMed]

27. Feldman, J.A.; Ballard, D.H. Modelos conexionistas y sus propiedades. *Cienc. Cogn.* **1982**, *6*, 205–254. [CrossRef]

28. Parker, A.J.; Newsome, W.T. Sense and the single neuron: Probing the physiology of perception. *Ann. Rev. Neurosci.* **1998**, *21*, 227–277. [CrossRef]

29. Moss, F.; Ward, L.M.; Sannita, W.G. Stochastic resonance and sensory information processing: A tutorial and review application. *Clin. Neurophysiol.* **2004**, *115*, 267–281. [CrossRef]

30. Bruce, I.C.; White, M.W.; Irlicht, L.S.; O'Leary, S.J.; Dynes, S.; Javel, E.; Clark, G.M. A stochastic model of the electrically stimulated auditory nerve: Single-pulse response. *IEEE Trans. Biomed. Eng.* **1999**, *46*, 617–629. [CrossRef]

31. Hecht, S.; Shlaer, S.; Pirenne, M.H. Energy, quanta and vision. *J. Gen. Physiol.* **1942**, *25*, 819–840. [CrossRef]

32. Johanson, R.S.; Vallbo, A.B. Skin mechanoreceptorsin the human hand: An inference of some population properties. In *Sensory Functions of the Skin in Primates*; Pergamon: Oxford, UK, 1976; pp. 171–184. [CrossRef]

33. Salzman, C.D.; Murasugui, C.M.; Britten, K.H.; Newsome, W.T. Microstimulation in visual area M.T.: Effects on direction discrimination performance. *J. Neurosci.* **1992**, *2*, 2331–2355. [CrossRef]

34. Hawkins, H.L.; Hillyard, S.A.; Luck, S.J.; Mouloua, M.; Downing, C.J.; Woodward, D.P. Visual attention modulates signal detectability. *J. Exp. Psychol. Hum. Percept. Perform.* **1990**, *16*, 802–811. [CrossRef]

35. Steinmetz, P.N.; Manwani, A.; Koch, C.; London, M.; Segev, I. Subthreshold voltage noise due to channel fluctuations in active neuronal membranes. *J. Comp. Neurosci.* **2000**, *9*, 133–148. [CrossRef]

36. Gummer, A.W. Postsynaptic inhibition can explain the concentration of short inter-spike-intervals in avian auditory nerve fibers. *Hear. Res.* **1991**, *55*, 231–243. [CrossRef]

37. Richter, C.P.; Sauer, G.; Hoidis, S.; Klinke, R. Development of activity patterns in auditory nerve fibres of pigeons. *Hear. Res.* **1996**, *95*, 77–86. [CrossRef] [PubMed]

38. Barlow, H.B.; Levick, W.R.; Yoon, M. Responses to single quanta of light in retinal ganglion cells of the cat. *Vis. Res.* **1971**, *11* (Suppl. S3), 87–101. [CrossRef] [PubMed]
39. Lowen, S.B.; Liebovitch, L.S.; White, J.A. Fractal ion channels behavior generates fractal firing patterns in neuronal models. *Phys. Rev. Lett. E* **1999**, *59*, 5970–5980. [CrossRef] [PubMed]
40. Durand, J. Electrophysiological and morphological properties of rat abducens motoneurones. *Exp Brain Res.* **1989**, *76*, 141–152. [CrossRef] [PubMed]
41. Darwin, C.; Kebler, L. *On the Origin of Species by Means of Natural Selection, or, the Preservation of Favoured Races in the Struggle for Life*; J. Murray: London, UK, 1859.
42. Burnet, F.M. A Modification of Jerne's Theory of Antibody Production using the Concept of Clonal Selection. *CA Cancer J. Clin.* **1976**, *26*, 119–121. [CrossRef]
43. Edelman, G.M. Neural Darwinism: Selection and reentrant signaling in higher brain function. *Neuron* **1993**, *10*, 115–125.
44. Garrett, D.D.; Samanez-Larkin, G.R.; MacDonald, S.W.; Lindenberger, U.; McIntosh, A.R.; Grady, C.L. Moment-to-moment brain signal variability: A next frontier in human brain mapping? *Neurosci. Biobehav. Rev.* **2013**, *37*, 610–624. [CrossRef]
45. Renart, A.; Machens, C.K. Variability in neural activity and behavior. *Curr. Opin. Neurobiol.* **2014**, *25*, 211–220. [CrossRef]